Title
The axon–glia unit in white matter stroke: Mechanisms of damage and recovery

Authors
Rosenzweig, Shira
Carmichael, S Thomas

Publication Date
2015-10-01

DOI
10.1016/j.brainres.2015.02.019

Peer reviewed

Title: Age-dependent exacerbation of white matter stroke outcomes: a role for oxidative damage and inflammatory mediators

Authors:

Shira Rosenzweig, PhD

shirarosen@ucla.edu , Phone: (310) 794-9691 Fax: (310) 825-0759

S. Thomas Carmichael, MD, PhD

SCarmichael@mednet.ucla.edu , Phone: (310) 206-0550

Affiliation and address:

David Geffen School of Medicine at UCLA

Department of neurology

710 Westwood Plaza

Los Angeles, CA 90095

Cover title: Age exacerbates outcomes in white matter stroke

Figures: Figure 1 (A,B,C,D), Figure 2 (A,B,C,D), Figure 3 (A,B,C), Figure 4 (A,B), Figure 5 (A,B,C), Figure 6 (A,B)

Keywords: Stroke, White Matter, Aging, Oligodendrocytes, Axonal degeneration, oxidative stress, inflammation.

Subject Codes: [44] Acute Cerebral Infarction, [46] Behavioral Changes and Stroke, [63] Pathology of Stroke

Word count: Title page: 119, Manuscript: 4467

Abstract

Background and Purpose--Subcortical white matter stroke (WMS) constitutes up to 30% of all stroke subtypes. Mechanisms of oligodendrocyte and axon injury and repair play a central role in the damage and recovery following this type of stroke, and a comprehensive study of these processes requires a specialized experimental model that is different from common large artery, "gray matter" stroke models. Diminished recovery from stroke in aged patients implies that damage and repair processes are affected by advanced age, but such effects have not been studied in WMS.

Methods--WMS was produced with focal microinjection of the vasoconstrictor L-NIO into the subcortical white matter ventral to the mouse forelimb motor cortex in young adult (2 months), middle aged (15 months) and aged mice (24 months).

Results--WMS produced localized oligodendrocyte cell death with higher numbers of apoptotic cells and greater oxidative damage in aged brains than in young-adult brains. Increased expression of MCP1 and TNFα in motor cortex neurons correlated with a more distributed microglial activation in aged brains 7 days after WMS. At 2 months aged mice displayed increased white matter atrophy and greater loss of corticostriatal connections compared to young-adult mice. Behavioral testing revealed an age-dependent exacerbation of forelimb motor deficits caused by the stroke, with decreased long-term functional recovery in aged animals.

Conclusions--Age has a profound effect on the outcome of WMS, with more prolonged cell death and oxidative damage, increased inflammation, greater secondary white matter atrophy and a worse behavioral effect in aged vs young-adult mice.

Introduction

Subcortical white matter stroke (WMS) constitutes up to 30% of all stroke subtypes [1, 2], and has devastating clinical consequences. These infarcts produce focal deficits with incomplete recovery and are the second leading cause of dementia[3, 4]. Despite an abundance of pre-clinical literature featuring animal models of large artery, "gray matter" stroke, there have been few studies of white matter repair and recovery. This limitation has been due to lack of an effective animal model of WMS.

In addition, most studies using models of ischemic stroke have been performed on young animals. Ischemic stroke occurs mostly in older individuals, and recovery in aged patients is diminished in comparison to young patients [5, 6]. Aged animals differ from young animals in their neurophysiology, and pathophysiological features of brain ischemia differ across the lifespan [7, 8]. Furthermore, re-myelination efficiency in white matter lesions decreases with age [9]. Thus, studies utilizing young animals to model ischemic stroke may have not fully estimated the effects of ischemia on brain tissue in aged subjects.

We have recently developed a model of subcortical stroke in white matter below the mouse forelimb motor cortex that models many aspects of this disease in humans. The model includes an induction of focal ischemia resulting in cell death and white matter destruction at the infarct core, and a peri-infarct zone of partial myelin, axon and oligodendrocyte loss [10, 11]. This model has been adapted here to study how the damage and functional consequences following white matter ischemia differ between the young and aged brain.

Methods

Mice

All experiments were performed in accordance with National Institutes of Health animal protection guidelines and were approved by the University of California at Los Angeles Animal Research Committee. 32 three-month old C57/BL6 mice (Jackson), 24 fifteen-month old and 28 twenty four- month old C57/BL mice (NIA) were used in this study. Cohorts of animals (*n* = 6-8 per group) survived to 1, 2, 7, and 56 days after stroke or sham procedure..

White Matter Stroke

White matter stroke was produced as described[10] with modifications. The vasoconstrictor N5-(1-Iminoethyl)-L-ornithine (L-NIO; 27mg/ml in sterile physiological saline; Millipore) was injected via micropippette through the cortex at an angle of 45° with a dorso-posterior to ventro-anterior injection path, into the white matter underlying the forelimb motor cortex. This procedure promotes intense vasoconstriction at the site of injection, leading to focal ischemia [10, 12]. Three injections (each of 200 nl L-NIO solution) were made in the following coordinates: A/P: +0.5, 0, -0.5, M/L: -0.96 (for all three injections), D/V: -1.2, -1.15, -1.1. The pipette was left *in situ* for 5 min post-injection to allow proper diffusion. Control animals underwent a sham procedure during which a craniotomy was done similarly to stroke animals, with no subsequent injections.

Tissue Processing, Microscopy and Stereology

The tissue was processed as described previously[10, 11] (See Supplementary Data for detailed staining methods, http://stroke.ahajournals.org). High-resolution confocal images and Z-stacks were acquired (Nikon C2 confocal system). Area measurements of the infarct core, Iba-1

positive cells, neutrophils and cell nuclei tagged by TUNEL were stereologically quantified using the optical fractionator probe and neuroanatomical quantification software (Stereoinvestigator, MBF Bioscience, Williston, VT). Striatal axonal projections stained with NF200 were quantified with intensity profiles generated by ImageJ software (NIH).

Behavior

Gate and forelimb function were assessed in the grid walking task and the pasta matrix task as described previously[13-17] (See Supplementary Data for detailed behavior methods, http://stroke.ahajournals.org).

Statistical Analysis

Mice were randomly allocated to treatment groups. All tests were analyzed blindly to stroke condition or age. The required number of animals per group was determined by a power analysis, with the expected variance and change in performance in the pasta matrix and grid-walking tasks predicted based on preliminary studies in young-adult animals. A group size of n=8 was predicted to be sufficient to detect a statistically significant result in ANOVA with $\alpha=0.05$ and power > 0.8. All data are expressed as mean ± SEM. For cell quantification, axonal degeneration, white matter measurements and behavioral testing, differences between age and treatment groups were analyzed using one-way or two-way Analysis of Variance (ANOVA) with level of significance set at $p<0.05$, with Tukey's HSD post-hoc analysis (Excel and SigmaStat).

Results

Infarct Volume, Oligodendrocyte Death and Oxidative Damage following White Matter Stroke

To assess the differences in initial tissue damage following WMS between the young and aged brain, animals from the two age groups were sacrificed 24 and 48 hours post-stroke. Infarct volume was similar 24 and 48 hours after WMS, and no difference was detected between young-adult and aged animals (Supplementary Figure I, $p>0.3$, $n=8$). TUNEL staining 24 hours after stroke revealed extensive cell death throughout the infarct core in young-adult as well as aged mice (Figure 1A). In both age groups the apoptotic cells were localized to the white matter lesion and were not detected in surrounding cortical areas, confirming the focal nature of this stroke type. The number of apoptotic cells did not differ significantly between young and aged animals at the 24h time point (Figure 1A and 1D; $p>0.1$, $n=8$). However, 48 hours after WMS the number of apoptotic cells was significantly higher in aged animals compared to young animals, resulting in a total higher number of apoptotic cells detected in aged animals (Figure1A and 1D; $p<0.01$, $n=8$; TUNEL positive cells over 48 hours equaled 924 ± 46 in young-adults, 1166 ± 52 in aged, $p<0.05$). Double immunostaining for TUNEL and the oligodendrocyte marker Olig2 confirmed that cell death was primarily induced in oligodendrocytes (Figure 1C). Staining for 8-hydroxydeoxyguanosine (8-OHdG) revealed cells positive for this oxidative DNA adduct within the lesion. Similarly to the observed pattern of apoptosis, there was no difference between the age groups in the number of cells displaying oxidative damage 24 hours after WMS, but the number was higher in aged animals 48 hours after stroke (Figure1C and 1D; $p<0.03$, $n=8$).

Inflammatory Mediators and Reactive Cells following White Matter Stroke

The inflammatory response to stroke was assessed at 24 hours and 7 days, the latter being a time of maximal microglia/macrophage response in young adults with a related WMS [11]. Ly6G (neutrophil) / Iba-1 (microglia/macrophage) staining 24 hours after WMS showed neutrophil infiltration in the infarct core and reactive microglia surrounding the lesion (Supplementary Figure II.A). The numbers of neutrophils and Iba-1 positive microglia were similar between the age groups (Supplementary Figure II.B, Iba-1 $p>0.3$, neutrophils $p>3$; $n=6$). 7 days following stroke a greater infiltration of activated microglia densely filled and surrounded the infarct core (Figure 2A). The density of Iba-1 positive cells in the lesion did not differ significantly between the age groups (Figure 2C; $p>0.2$, $n=8$). Interestingly, while the increase in Iba-1 staining following stroke in young animals was limited to the infarct area, in aged animals there was a higher density of Iba-1 positive cells throughout the motor cortex compared to aged controls and young stroke animals (Figure 2B and 2D; control young-adult vs. aged $p<0.05$, WMS young-aged vs. aged $p<0.005$, control aged vs. WMS aged $p<0.01$, $n=8$).

To test whether upregulation of inflammatory mediators could have contributed to microglial activation in the cortex, expression of monocyte chemotactic protein-1 (MCP1) and the pro-inflammatory cytokine TNFα was measured. 7 days after stroke there was a robust MCP1 expression in reactive astrocytes in or around the infarct core (Supplementary Figure III.A). The number of MCP1-positive astrocytes did not differ between age groups (Supplementary Figure III.B, $p>0.3$, $n=6$). Interestingly, MCP1 could be transiently detected in a subset of motor cortex neurons only in aged brains 24 hours after stroke. Neuronal expression of MCP1 was not present in stroked young-adult animals or control animals of either age group, and was undetectable in

stroked aged brains by day 7 (Figure 3C). At 7 days, TNFα was expressed in neurons in cortical areas adjacent to the stroke lesion in both young-adult and aged mice (Figure 3A). When quantified in three regions at increasing distances from the infarct core, TNFα-positive neurons were more numerous and extended further away from the infarct core in aged brains compared to young-adult brains (Figure 3B, $p>0.2$ in region 0-300um, $p<0.01$ in regions 300-400um and 400-500um, young-adult WMS vs. aged WMS; $n=6$).

Long-Term Tissue Outcome of White Matter Stroke: myelin loss and axonal degeneration

Immunostaining for myelin basic protein (MBP) revealed an area of myelin loss in the infarct core, and a narrowing of the white matter medial to the stroke site at late time points after stroke (56 days, Figure 4). To quantify this volume change, the thickness of the white matter was measured at 10 equal increments from the midline (1) to the center of the infarct lesion (or equivalent point in controls – 10). A local decrease in the thickness of the white matter following stroke was observed in both young-adult and aged animals. However, it was markedly more pronounced in aged animals (Figure 4B, young-adult WMS vs. control $p<0.04$ at interval #8, aged WMS vs. control $p<0.005$ at intervals #6-9, WMS young-adult vs. aged $p<0.009$ at intervals #6-9, $n=8$).

Immunostaining for the axonal marker NF200 revealed that the loss of myelin in the white matter was accompanied by loss of axonal projections from the cortex to the dorsomedial striatum after stroke. These axonal bundles include corticostriatal projections from the ipsi- and contralateral cortex that play an important part in controlling motor programs and movement [18]. Quantification of axonal staining in the region of corticostriatal projections (See Supplementary

Data for detailed axonal measurement methods, http://stroke.ahajournals.org) indicated a loss of axonal bundles at late time points after stroke that was more pronounced in aged animals compared to young animals (Figure 5C; young-adult WMS $p<0.04$ compared to control, aged WMS $p<0.01$ compared to control, aged WMS $p<0.03$ compared to young-adult WMS, $n=8$).

Functional Impairments following White Matter Stroke

To test whether the greater degenerative loss of white matter tracts and corticostriatal projections in aged WMS correlated with functional impairments, the baseline performance of young-adult and aged mice was assessed before and after stroke in two behavioral tasks that rely on forelimb motor control. A third, middle-aged group of animals was similarly tested in these tasks, to better evaluate whether the effect of age on functional impairment is graded with advancing age.

The pasta matrix reach task is specifically aimed at evaluating strength, reach capacity and dexterity of the mouse forelimb [14, 19, 20]. Baseline performance in the pasta matrix reach task was similar across the three age groups (Supplementary Figure IV.A, $p>0.1$, $n=8$). Following WMS, there was a significant decrease in performance in all age groups, but middle-aged and aged mice performed significantly worse than young-adult mice (Figure 6A; week 1 post stroke performance was 62.2±11.3% of baseline in young adults, 41.1±5.7% in middle-aged and 48.2±5.7% in aged, $p<0.02$, $n=8$). Functional recovery and return to baseline performance levels were observed in young-adult animals starting 4 weeks post-stroke (Figure. 6A, left; $p<0.05$ weeks 1-3, $p>0.1$ weeks 4-8, $n=8$), and in middle-aged animals 6 weeks post-stroke (Figure 6A, middle; $p<0.005$ weeks 1-5, $p>0.06$ weeks 6-8, $n=8$). In contrast, no improvement in

performance was observed in aged animals throughout the 8 weeks of testing (Figure 6A, right; $p<0.001$ weeks 1-8, $n=8$).

Similarly to the pasta matrix reach task, there were no differences between age groups in baseline performance in the grid-walking task (Supplementary Figure IV.B, $p>0.3$, $n=8$). Analysis of forelimb footfaults revealed a significant increase in the number of footfaults recorded in middle-aged and aged, but not young-adult mice, following WMS (Figure 6B; 7 days post stroke, young adults $p>0.3$, middle-aged $p<0.005$, aged $p<0.01$, $n=8$). 8 weeks following stroke, there was a functional recovery and return to baseline performance levels in middle-aged mice, but not aged mice (Figure 6B middle, right; 56 days post stroke, middle-aged $p>0.1$, aged $p<0.01$, $n=8$). These behavioral results indicate an age-related worsening of initial motor performance after stroke and a decline in recovery with age.

Discussion

In the aged brain white matter stroke produces more prolonged oligodendrocyte cell death and oxidative damage, more distributed microglial activation and expression of cytokines MCP1 and TNFα, increased white matter atrophy and greater loss of corticostriatal connections compared to the young-adult brain. When comparing young-adult, middle-aged and aged animals, stroke has an age dose-response, with progressively greater functional impairment and a greater initial behavioral deficit from young adult to middle aged and then aged animals.

The greater oligodendrocyte death and oxidative damage in aged animals despite a similar areal extent of the lesion across age groups may be caused by the ischemic injury and oxidative stress that follow white matter stroke and are more severe in aged animals[21]. The axons in the white matter contain abundant mitochondria, a main source of reactive oxygen species following ischemia[22]. Mitochondrial activity and integrity decline during aging, and endogenous antioxidant system activities exhibit an age-dependent decline [23, 24]. Both processes may contribute to an increased susceptibility to ischemia, making mitochondria-mediated oxidative stress a predominant pathway of white matter injury in the aged brain[7].

The increase in oligodendrocyte cell death following stroke in aged animals likely contributes to axonal degeneration through secondary demyelination. Loss of normal myelination leads to damage in axonal integrity and dysfunction [25, 26]. In addition, the ischemic insult has a direct effect on axons that may be more severe or occur through distinct mechanisms in aged animals compared with young animals [21, 27]. The present data show that a greater sensitivity of myelinated axons to ischemia is not reflected in an initially larger infarct zone in WMS, but in a substantially greater secondary loss of these axons with age.

There is an age-specific induction of several interacting arms of neuroinflammation following WMS. In the aged brain WMS induces MCP-1 and TNFα in neurons distant to the infarct but whose axons project through the ischemic area. Such a remote neuronal induction of MCP1 to axonal injury has been reported in nerve axotomy [28]. These two cytokines attract and activate microglia and macrophages[29], and may underlie the larger numbers of microglia/macrophages found in the cortical regions above a WMS in the aged brain. TNFα induces a more injurious

response in tissue macrophages[30], greater damage to myelin and oligodendrocytes[31], and can result in greater injury in hypoxic central and peripheral insults [32, 33]. A more widespread and damaging inflammatory response in the cortex of aged animals has been reported in other models of injury, such as chronic stress or systemic LPS injection [34, 35].

The observed loss of corticostriatal projections likely underlies, at least in part, the motor impairment observed in this WMS model. The greater impairment observed in middle-aged and aged mice in the first weeks following stroke, and the diminished functional recovery in aged mice at longer time points, can be attributed respectively to greater initial damage and inefficient repair processes that result in lasting white matter atrophy. In addition to a more efficient white matter repair process in young brains, the behavioral recovery observed 4 weeks following stroke in young-adult mice, and 6-8 weeks following stroke in middle-aged mice, may be achieved through axonal sprouting and formation of new patterns of neuronal connections in adjacent brain regions [36, 37]. The gene expression profile that drives this reorganization differs significantly between the young and aged brain [38], and this may further contribute to the diminished recovery after WMS in aged animals.

In summary, white matter stroke causes increased inflammation, oxidative tissue injury and delayed white matter atrophy in aged animals, which translate into an age-dependent exacerbation of behavioral motor deficits. The use of a clinically-relevant model is likely crucial in translational research aimed at developing therapeutic interventions for WMS. The present studies utilize an extensive and long-duration multimodal analysis of the cellular and behavioral

phenotypes of WMS in the aged brain, setting the stage for future pharmacological approaches to mitigate this progressive damage.

Sources of Funding:

This work was supported by National Institutes of Health (NIH) grant RO1 NS071481 (Dr. Carmichael).

Acknowledgments:

We thank Michael Reitman, Wenli Mui and Meghan Yetzke for excellent technical assistance.

Disclosures: None.

References

1. Bamford J, Sandercock P, Dennis M, Burn J, Warlow C. Classification and natural history of clinically identifiable subtypes of cerebral infarction. *Lancet*. 1991;337:1521-1526
2. Schneider AT, Kissela B, Woo D, Kleindorfer D, Alwell K, Miller R, et al. Ischemic stroke subtypes: A population-based study of incidence rates among blacks and whites. *Stroke; a journal of cerebral circulation*. 2004;35:1552-1556
3. Chui HC. Subcortical ischemic vascular dementia. *Neurologic clinics*. 2007;25:717-740, vi

4. Srikanth V, Beare R, Blizzard L, Phan T, Stapleton J, Chen J, et al. Cerebral white matter lesions, gait, and the risk of incident falls: A prospective population-based study. *Stroke; a journal of cerebral circulation*. 2009;40:175-180

5. Bousser MG. Stroke prevention: An update. *Frontiers of medicine*. 2012;6:22-34

6. Ovbiagele B, Nguyen-Huynh MN. Stroke epidemiology: Advancing our understanding of disease mechanism and therapy. *Neurotherapeutics : the journal of the American Society for Experimental NeuroTherapeutics*. 2011;8:319-329

7. Li N, Kong X, Ye R, Yang Q, Han J, Xiong L. Age-related differences in experimental stroke: Possible involvement of mitochondrial dysfunction and oxidative damage. *Rejuvenation research*. 2011;14:261-273

8. Popa-Wagner A, Badan I, Walker L, Groppa S, Patrana N, Kessler C. Accelerated infarct development, cytogenesis and apoptosis following transient cerebral ischemia in aged rats. *Acta neuropathologica*. 2007;113:277-293

9. Sim FJ, Zhao C, Penderis J, Franklin RJ. The age-related decrease in cns remyelination efficiency is attributable to an impairment of both oligodendrocyte progenitor recruitment and differentiation. *The Journal of neuroscience : the official journal of the Society for Neuroscience*. 2002;22:2451-2459

10. Hinman JD, Rasband MN, Carmichael ST. Remodeling of the axon initial segment after focal cortical and white matter stroke. *Stroke; a journal of cerebral circulation*. 2013;44:182-189

11. Sozmen EG, Kolekar A, Havton LA, Carmichael ST. A white matter stroke model in the mouse: Axonal damage, progenitor responses and mri correlates. *Journal of neuroscience methods*. 2009;180:261-272

12. Horie N, Maag AL, Hamilton SA, Shichinohe H, Bliss TM, Steinberg GK. Mouse model of focal cerebral ischemia using endothelin-1. *Journal of neuroscience methods*. 2008;173:286-290

13. Tennant KA, Adkins DL, Scalco MD, Donlan NA, Asay AL, Thomas N, et al. Skill learning induced plasticity of motor cortical representations is time and age-dependent. *Neurobiology of learning and memory*. 2012;98:291-302

14. Tennant KA, Jones TA. Sensorimotor behavioral effects of endothelin-1 induced small cortical infarcts in c57bl/6 mice. *Journal of neuroscience methods*. 2009;181:18-26

15. Clarkson AN, Huang BS, Macisaac SE, Mody I, Carmichael ST. Reducing excessive gaba-mediated tonic inhibition promotes functional recovery after stroke. *Nature*. 2010;468:305-309

16. Clarkson AN, Overman JJ, Zhong S, Mueller R, Lynch G, Carmichael ST. Ampa receptor-induced local brain-derived neurotrophic factor signaling mediates motor recovery after stroke. *The Journal of neuroscience : the official journal of the Society for Neuroscience*. 2011;31:3766-3775

17. Overman JJ, Clarkson AN, Wanner IB, Overman WT, Eckstein I, Maguire JL, et al. A role for ephrin-a5 in axonal sprouting, recovery, and activity-dependent plasticity after stroke. *Proceedings of the National Academy of Sciences of the United States of America*. 2012;In press.

18. Reiner A, Hart NM, Lei W, Deng Y. Corticostriatal projection neurons - dichotomous types and dichotomous functions. *Frontiers in neuroanatomy*. 2010;4:142

19. Teskey GC, Flynn C, Goertzen CD, Monfils MH, Young NA. Cortical stimulation improves skilled forelimb use following a focal ischemic infarct in the rat. *Neurological research*. 2003;25:794-800

20. Chiken S, Tokuno H. Impairment of skilled forelimb use after ablation of striatal interneurons expressing substance p receptors in rats: An analysis using a pasta matrix reaching task. *Experimental brain research. Experimentelle Hirnforschung. Experimentation cerebrale*. 2005;162:532-536

21. Baltan S. Ischemic injury to white matter: An age-dependent process. *The Neuroscientist : a review journal bringing neurobiology, neurology and psychiatry*. 2009;15:126-133

22. Lipton P. Ischemic cell death in brain neurons. *Physiological reviews*. 1999;79:1431-1568

23. Tian L, Cai Q, Wei H. Alterations of antioxidant enzymes and oxidative damage to macromolecules in different organs of rats during aging. *Free radical biology & medicine*. 1998;24:1477-1484

24. Kwong LK, Sohal RS. Age-related changes in activities of mitochondrial electron transport complexes in various tissues of the mouse. *Archives of biochemistry and biophysics*. 2000;373:16-22

25. Tekkok SB, Goldberg MP. Ampa/kainate receptor activation mediates hypoxic oligodendrocyte death and axonal injury in cerebral white matter. *The Journal of neuroscience : the official journal of the Society for Neuroscience*. 2001;21:4237-4248

26. Edgar JM, Nave KA. The role of cns glia in preserving axon function. *Current opinion in neurobiology*. 2009;19:498-504

27. Matute C, Domercq M, Perez-Samartin A, Ransom BR. Protecting white matter from stroke injury. *Stroke; a journal of cerebral circulation*. 2012

28. Flugel A, Hager G, Horvat A, Spitzer C, Singer GM, Graeber MB, et al. Neuronal mcp-1 expression in response to remote nerve injury. *Journal of cerebral blood flow and metabolism : official journal of the International Society of Cerebral Blood Flow and Metabolism*. 2001;21:69-76

29. Yoshizato K, Kuratsu J, Takeshima H, Nishi T, Yoshimura T, Ushio Y. Increased monocyte chemoattractant protein-1 expression by tumor necrosis factor-alpha can mediate macrophage infiltration in gliomas. *International journal of oncology*. 1996;8:493-497

30. Riches DW, Chan ED, Winston BW. Tnf-alpha-induced regulation and signalling in macrophages. *Immunobiology*. 1996;195:477-490

31. Selmaj KW, Raine CS. Tumor necrosis factor mediates myelin and oligodendrocyte damage in vitro. *Annals of neurology*. 1988;23:339-346

32. Smith RM, McCarthy J, Sack MN. Tnf alpha is required for hypoxia-mediated right ventricular hypertrophy. *Molecular and cellular biochemistry*. 2001;219:139-143

33. Lambertsen KL, Biber K, Finsen B. Inflammatory cytokines in experimental and human stroke. *Journal of cerebral blood flow and metabolism : official journal of the International Society of Cerebral Blood Flow and Metabolism*. 2012;32:1677-1698

34. Buchanan JB, Sparkman NL, Chen J, Johnson RW. Cognitive and neuroinflammatory consequences of mild repeated stress are exacerbated in aged mice. *Psychoneuroendocrinology*. 2008;33:755-765

35. Henry CJ, Huang Y, Wynne AM, Godbout JP. Peripheral lipopolysaccharide (lps) challenge promotes microglial hyperactivity in aged mice that is associated with exaggerated induction of both pro-inflammatory il-1beta and anti-inflammatory il-10 cytokines. *Brain, behavior, and immunity*. 2009;23:309-317

36. Carmichael ST. Cellular and molecular mechanisms of neural repair after stroke: Making waves. *Annals of neurology*. 2006;59:735-742

37. Carmichael ST, Wei L, Rovainen CM, Woolsey TA. New patterns of intracortical projections after focal cortical stroke. *Neurobiology of disease*. 2001;8:910-922

38. Li S, Overman JJ, Katsman D, Kozlov SV, Donnelly CJ, Twiss JL, et al. An age-related sprouting transcriptome provides molecular control of axonal sprouting after stroke. *Nature neuroscience*. 2010;13:1496-1504

Figure Legends

Figure 1. Apoptotic cell death and oxidative damage following white matter stroke**.** TUNEL-positive cells (green) localized to the infarct core 24 and 48 hours after stroke. Cell nuclei stained with propidium iodide (red). Scale bar = 200μm (**A**). 8-OHdG-positive cells (red) localized to the infarct core 24 and 48 hours after stroke. Cell nuclei stained with DAPI (blue). Scale bar = 100μm (**A**). TUNEL-positive cells (green, arrows) express the oligodendrocyte marker Olig2 (red). Scale bar = 50μm (**C**). At 48 hours there is a significant increase in the number of apoptotic cells and cells displaying oxidative damage in aged versus young-adult (**D**). *$p<0.03$, ** $p<0.01$.

Figure 2. Reactive microglia in the infarct core and motor cortex. White matter stroke lesions are densely filled with Iba-1-positive microglia (red) 7 days following stroke. Cell nuclei stained with DAPI (blue). Scale bar = 100μm (**A**). Iba-1 positive microglia (red) are more extensive in the motor cortex of aged animals. Scale bar = 25μm (**B**). There is no difference in Iba-1-positive cell number in white matter stroke lesions (**C**) but an increase in motor cortex of aged mice (**D**). *p<0.05, vs. control young-adult ***p<0.005, vs. young-adult WMS, #p<0.01 aged control vs. aged WMS.

Figure 3. Expression of inflammatory mediators in neurons. TNFα expression (red) in neurons (NeuN, green) adjacent and distant from the infarct core (A). TNFα-positive neurons were more numerous and extended further away from the infarct core in aged brains compared to young-adult brains (B). MCP1 expression (red) in motor cortex neurons (NeuN, green) 24 hours after WMS (C). **p<0.01, vs. young-adult WMS at same region.

Figure 4. White matter atrophy 8 weeks after WMS. MBP staining shows loss of myelin in the infarct core (asterisk) and a narrowing of the white matter medial to the stroke (arrow) which is more pronounced in aged animals (bottom) (**A**). The width of the white matter measured at 10 equal intervals from midline to stroke shows a significant atrophy in aged mice. The change is expressed as a percentage of midline width (**B**). *p<0.04 young-adults WMS vs. controls, ###p<0.005 aged WMS vs. controls, Ħ p<0.01 aged WMS vs. young-adult WMS.

Figure 5. Loss of corticostriatal projections. NF200 staining shows loss of axons descending from the cortex into the dorso-medial striatum. The Intensity was quantified in a 0.5x0.7mm area

(outlined) (**A**). The corresponding plot profiles (**B**) show staining intensity (grey values) in each column of pixels from medial (left of graph) to lateral (right of graph) in the region outlined in (A). The cumulative intensity of NF200 in the regions of interest shows a significant decline in aged animals after WMS (**C**). *$p<0.04$, **$p<0.01$ compared to age-matched controls. #$p<0.03$ aged WMS vs. young-adult WMS.

Figure 6. Behavioral deficits following WMS. Performance in the pasta matrix reach task was impaired following WMS, with greater impairment in middle-aged (middle) and aged (right) mice, and no functional recovery in aged mice. (**A**).Performance in the grid walking task was impaired following WMS only in middle-aged (middle) and aged (right) mice. There was no recovery in aged mice (**B**). *$p<0.05$, **$p<0.01$, ***$p<0.005$.

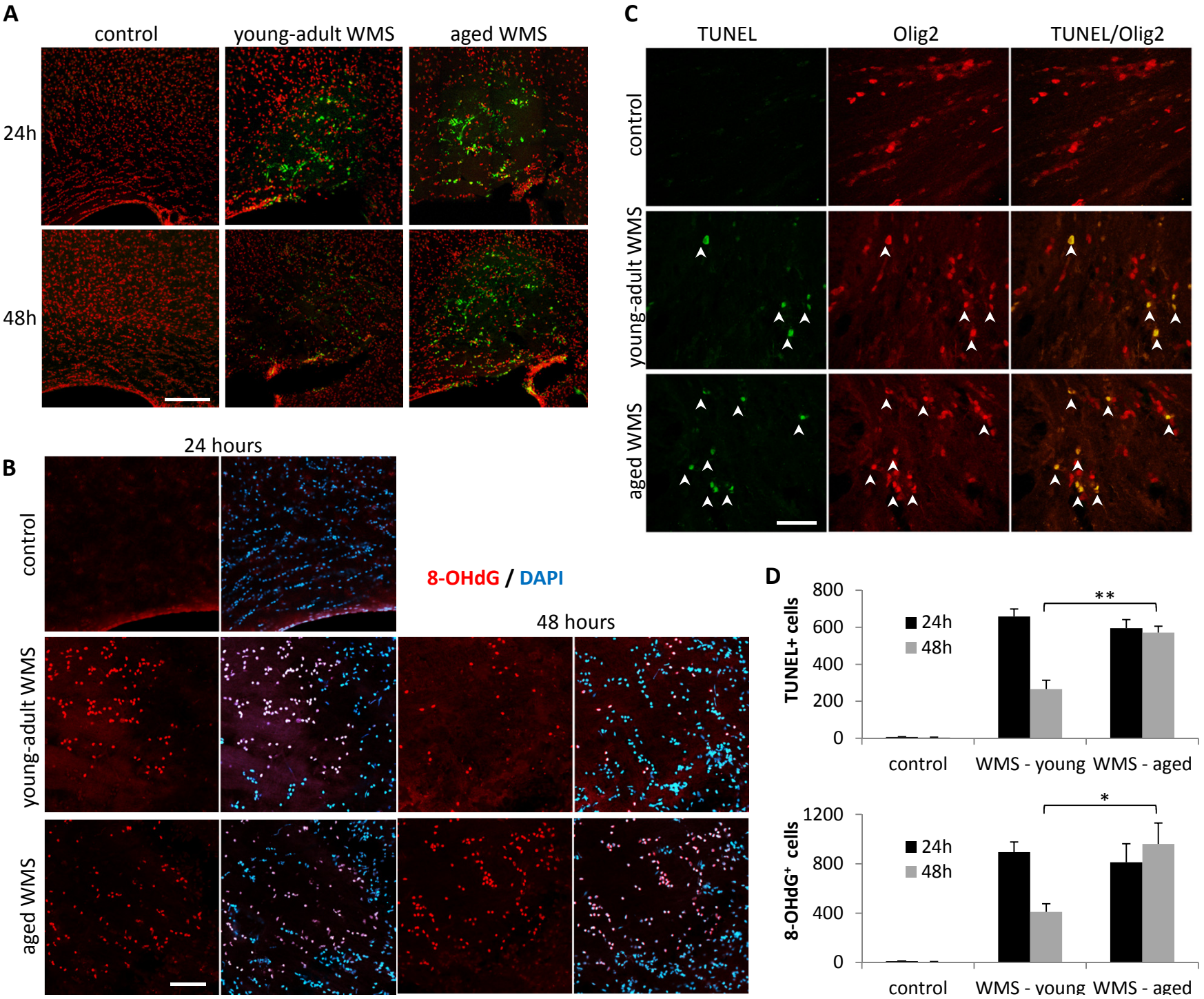
A
control
young-adult WMS
aged WMS
24h
48h
B
24 hours
48 hours
control
young-adult WMS
aged WMS
8-OHdG / DAPI
C
TUNEL
Olig2
TUNEL/Olig2
control
young-adult WMS
aged WMS
D
TUNEL+ cells
800
600
400
200
0
24h
48h
**
control
WMS - young
WMS - aged
8-OHdG+ cells
1200
800
400
0
24h
48h
*
control
WMS - young
WMS - aged

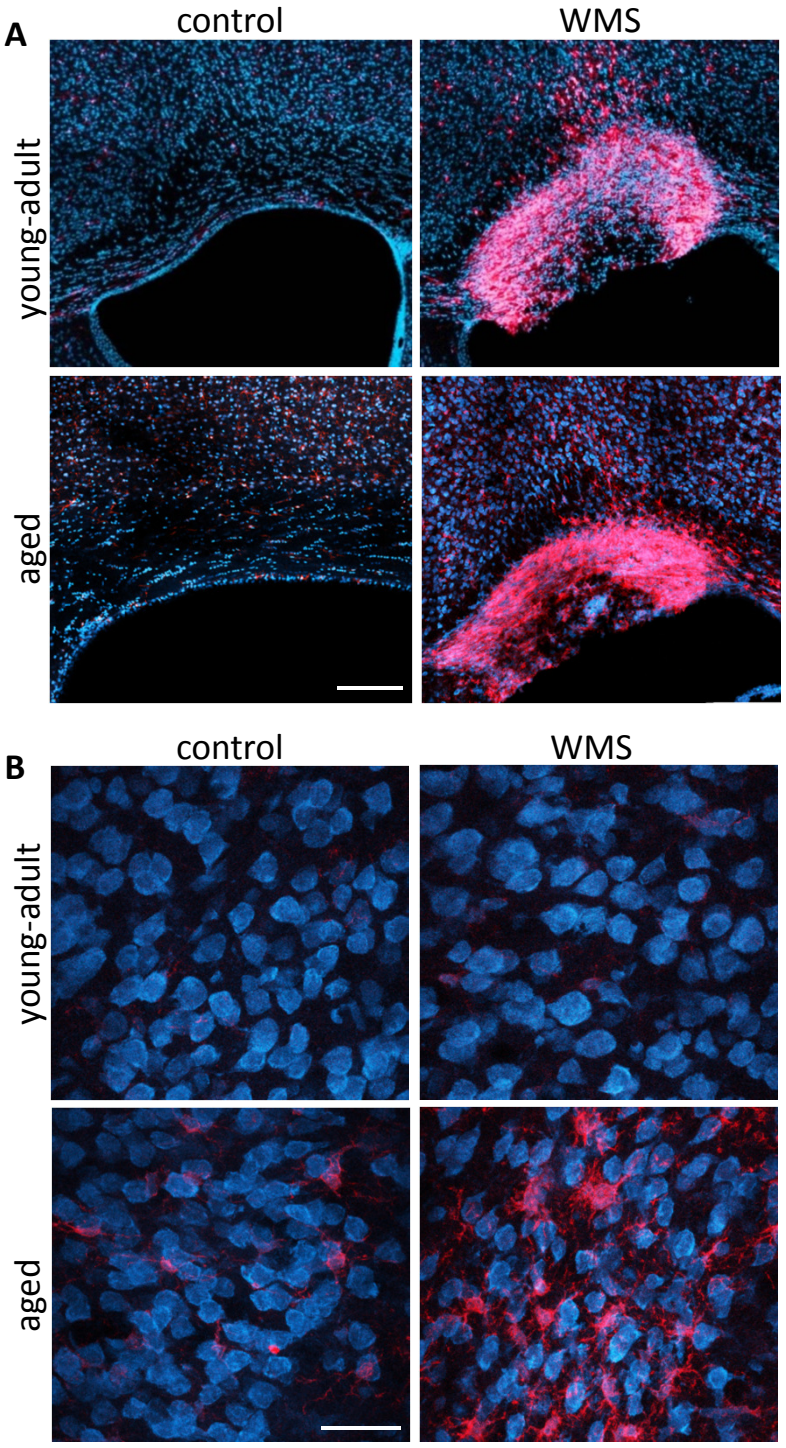
A
control
WMS
young-adult
aged
B
control
WMS
young-adult
aged

Figure 2

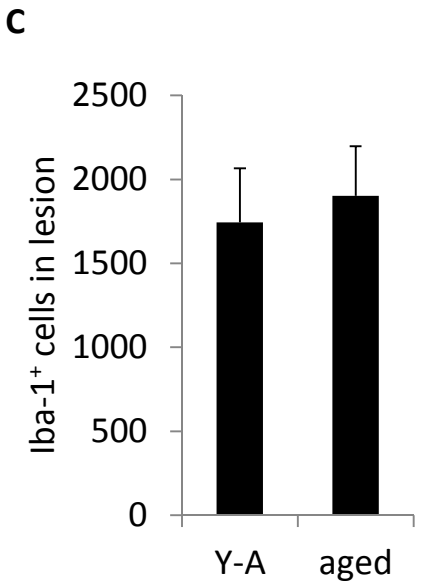
C
Iba-1⁺ cells in lesion
2500
2000
1500
1000
500
0
Y-A
aged

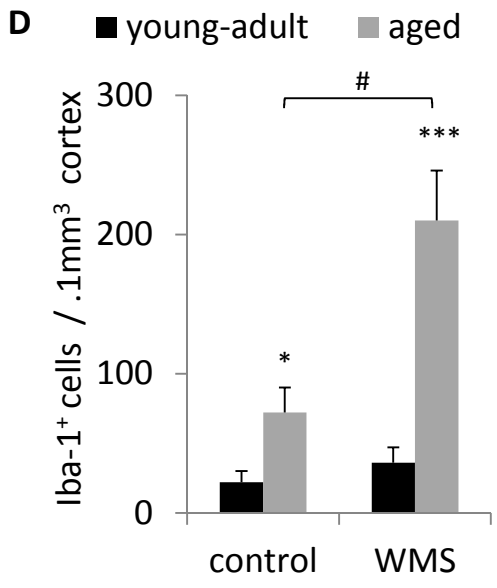
D
young-adult
aged
Iba-1⁺ cells / .1mm³ cortex
300
200
100
0
#
***
*
control
WMS

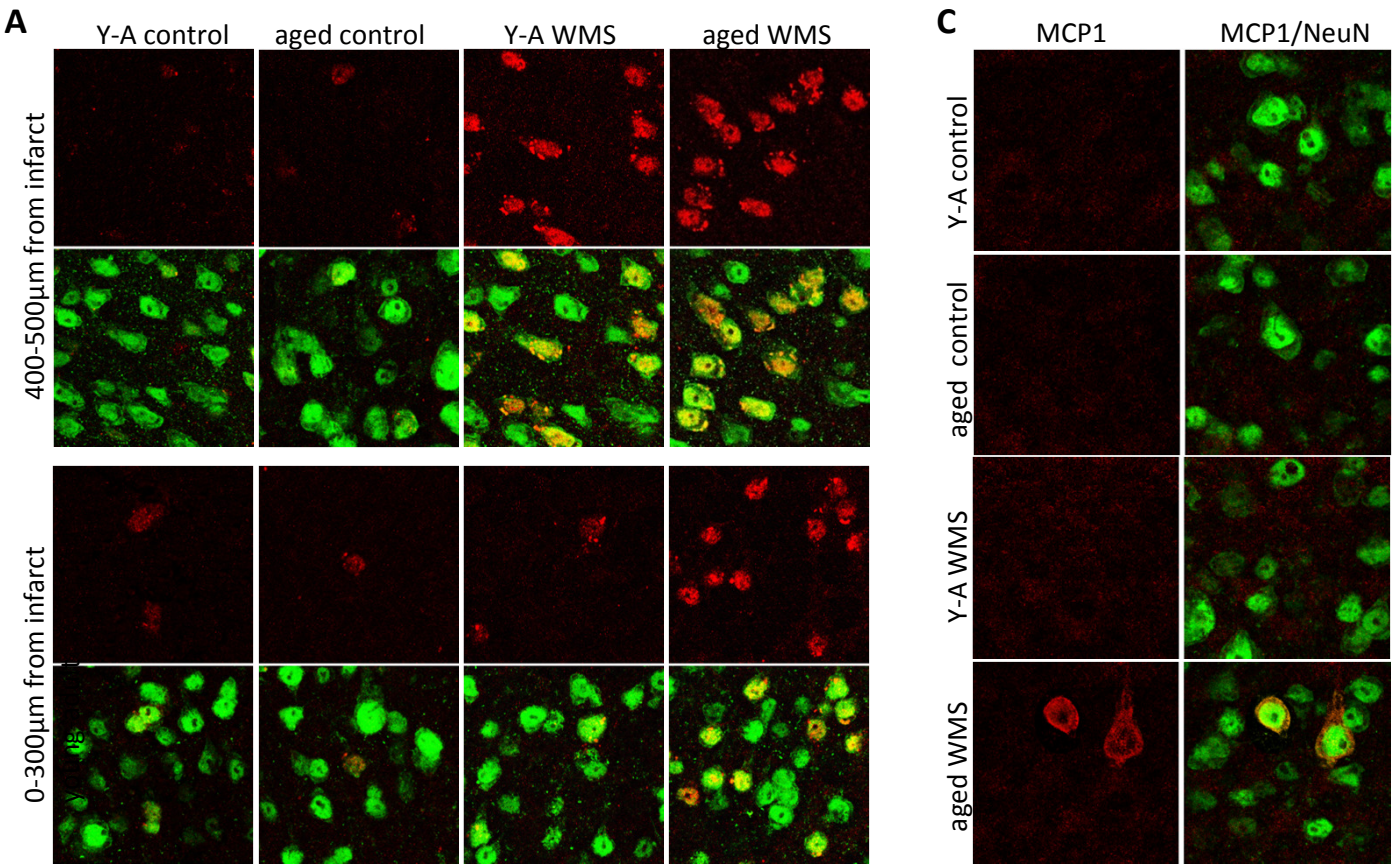
A
Y-A control
aged control
Y-A WMS
aged WMS
400-500µm from infarct
0-300µm from infarct
C
MCP1
MCP1/NeuN
Y-A control
aged control
Y-A WMS
aged WMS

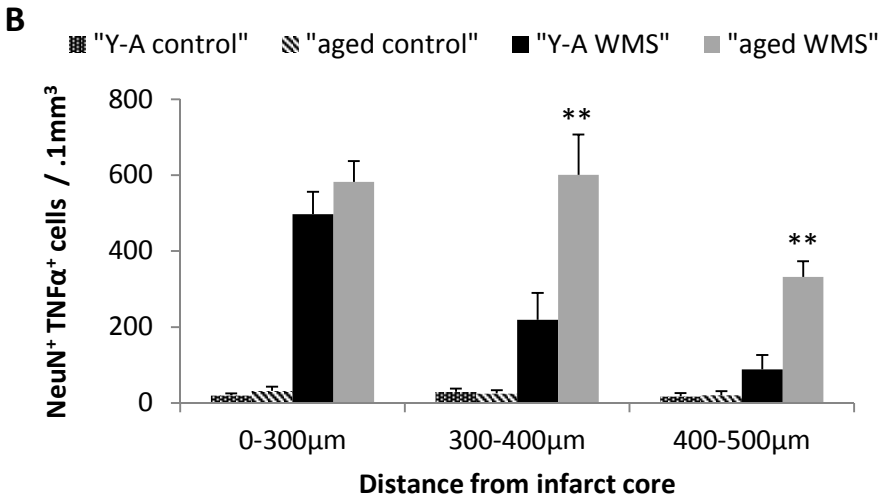
B
"Y-A control"
"aged control"
"Y-A WMS"
"aged WMS"
NeuN⁺ TNFα⁺ cells / .1mm³
800
600
400
200
0
**
**
0-300µm
300-400µm
400-500µm
Distance from infarct core

Figure 3

Figure 4

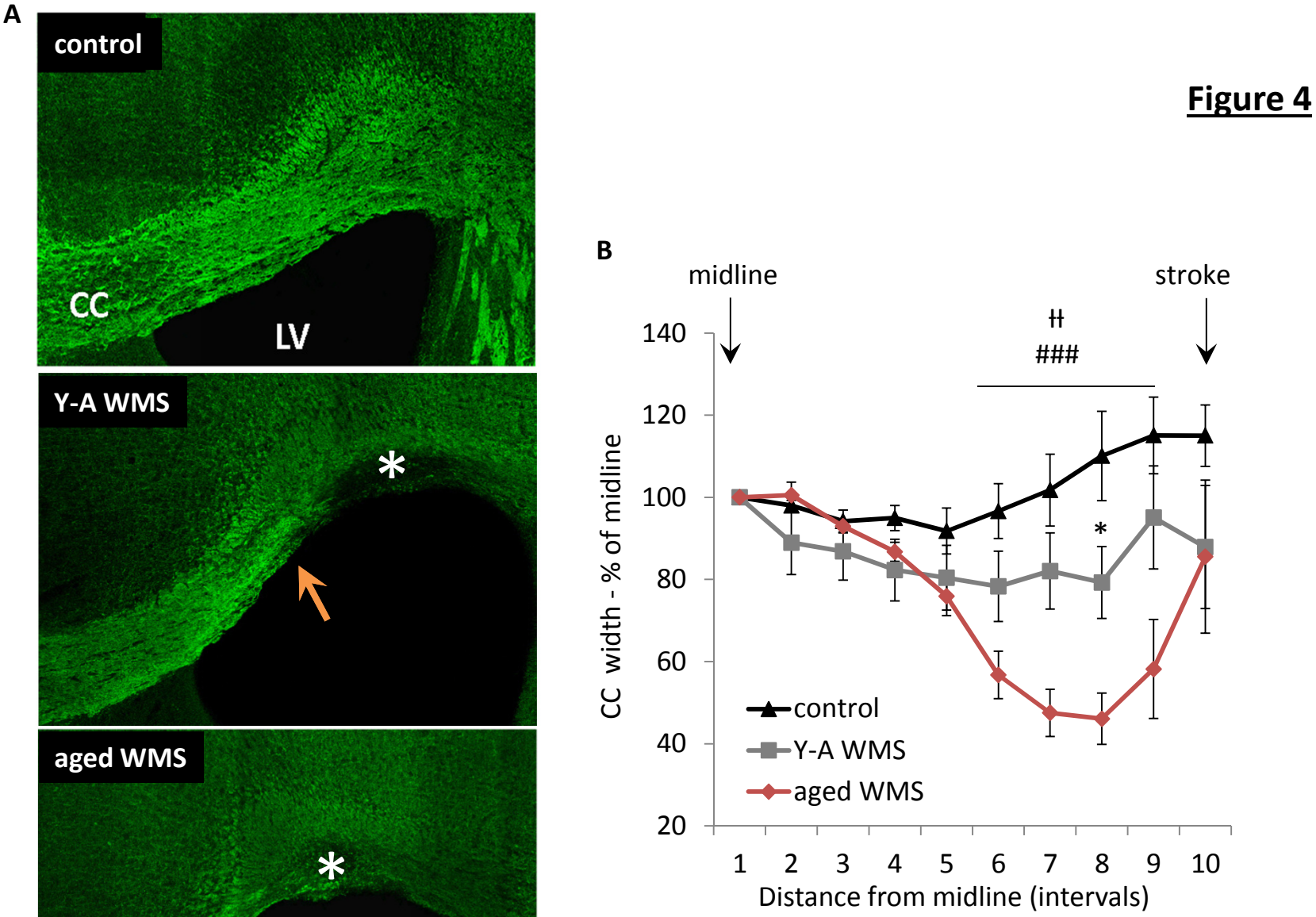
A
control
CC
LV
Y-A WMS
*
aged WMS
*
B
midline
stroke
ǂ
###
140
120
100
80
60
40
20
CC width - % of midline
*
control
Y-A WMS
aged WMS
1
2
3
4
5
6
7
8
9
10
Distance from midline (intervals)

Figure 5

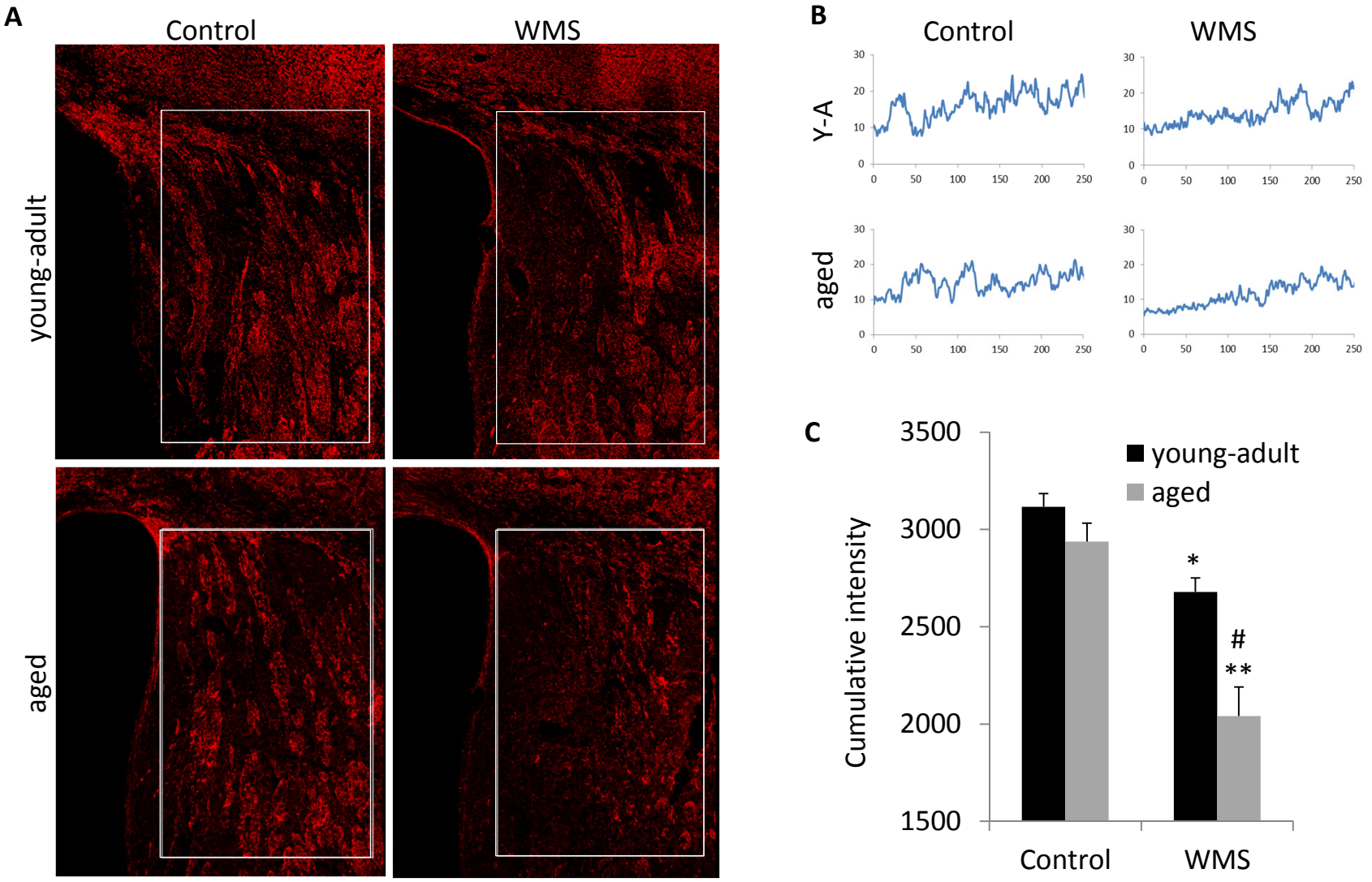
A
Control
WMS
young-adult
aged
B
Control
WMS
Y-A
aged
0
10
20
30
0
50
100
150
200
250
C
Cumulative intensity
3500
3000
2500
2000
1500
young-adult
aged
*
#
**
Control
WMS

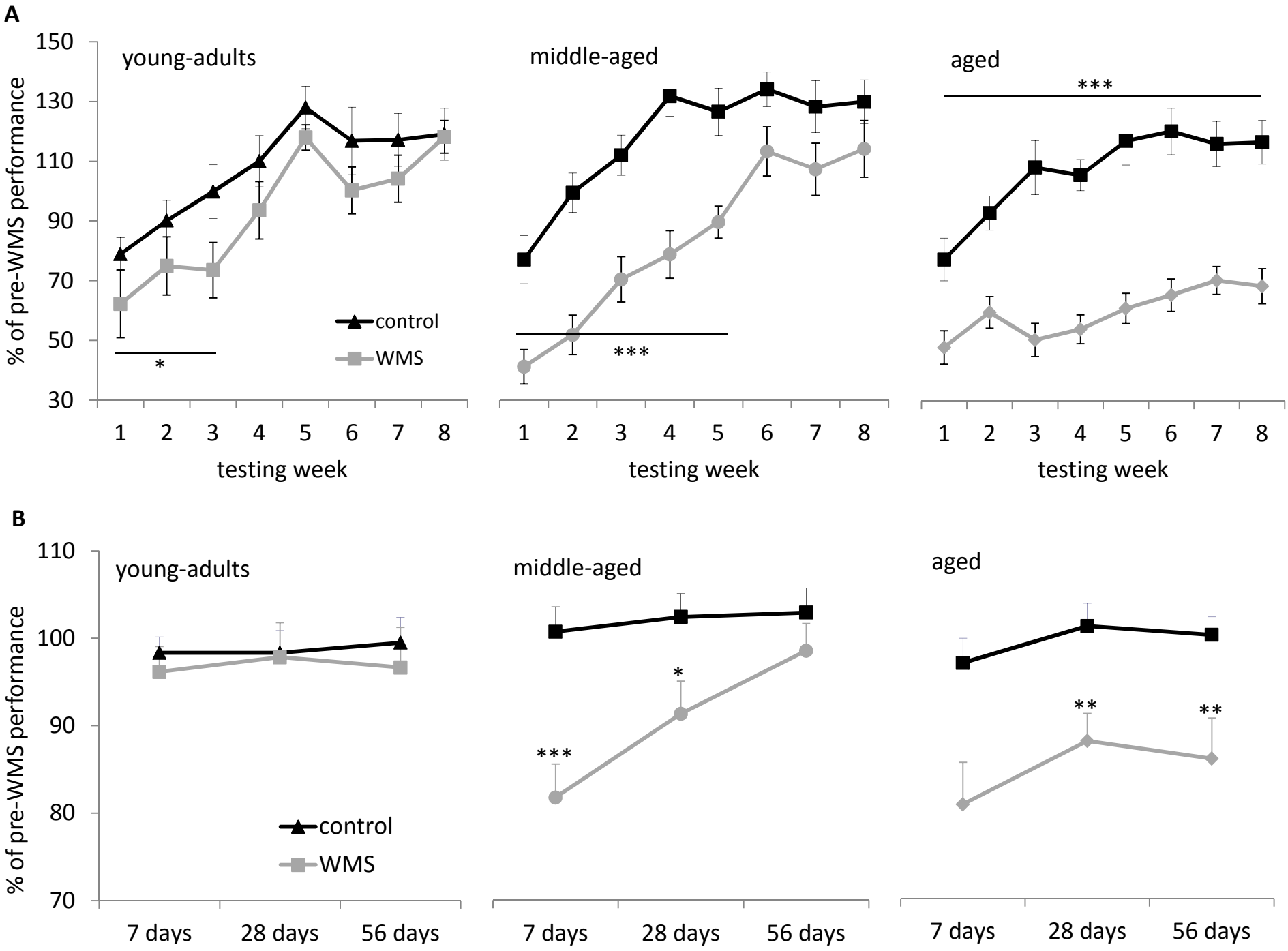
A
young-adults
middle-aged
aged
% of pre-WMS performance
150
130
110
90
70
50
30
control
WMS
*
***
***
1 2 3 4 5 6 7 8
testing week
B
young-adults
middle-aged
aged
% of pre-WMS performance
110
100
90
80
70
control
WMS
***
*
**
**
7 days
28 days
56 days

Supp. Fig 1

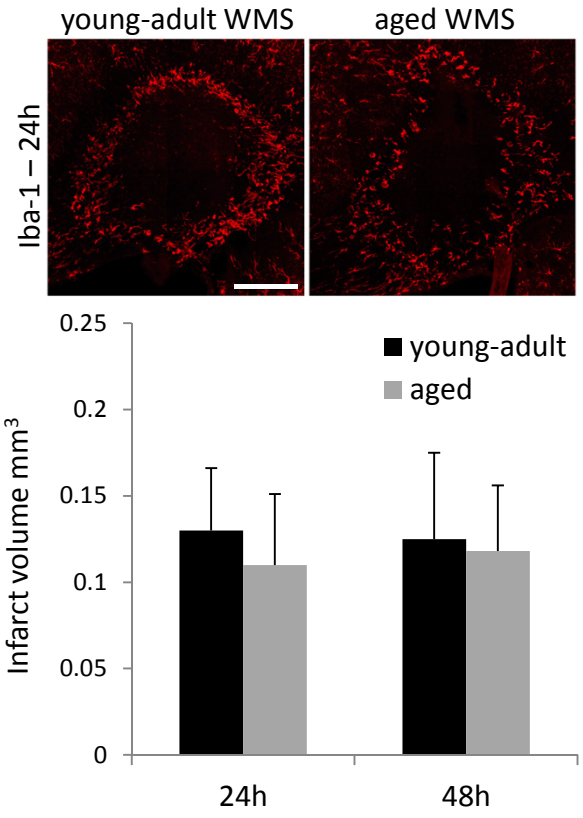

Supp. Fig 2

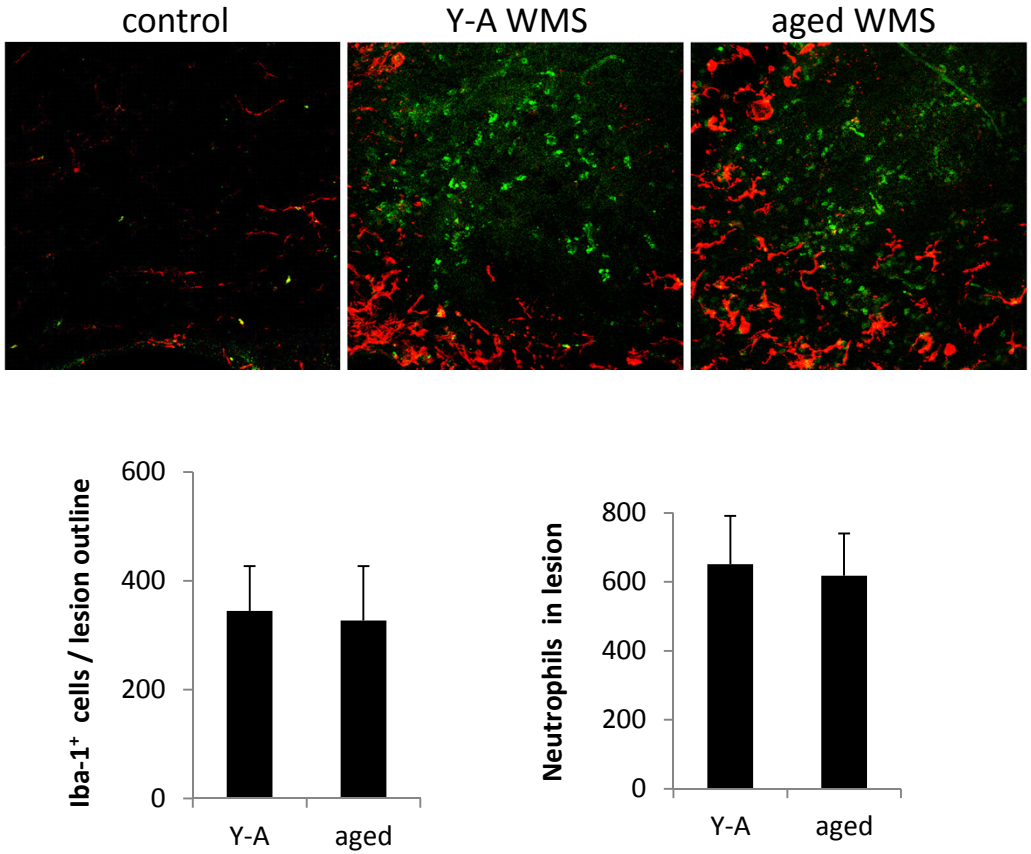

Supp. Fig 3

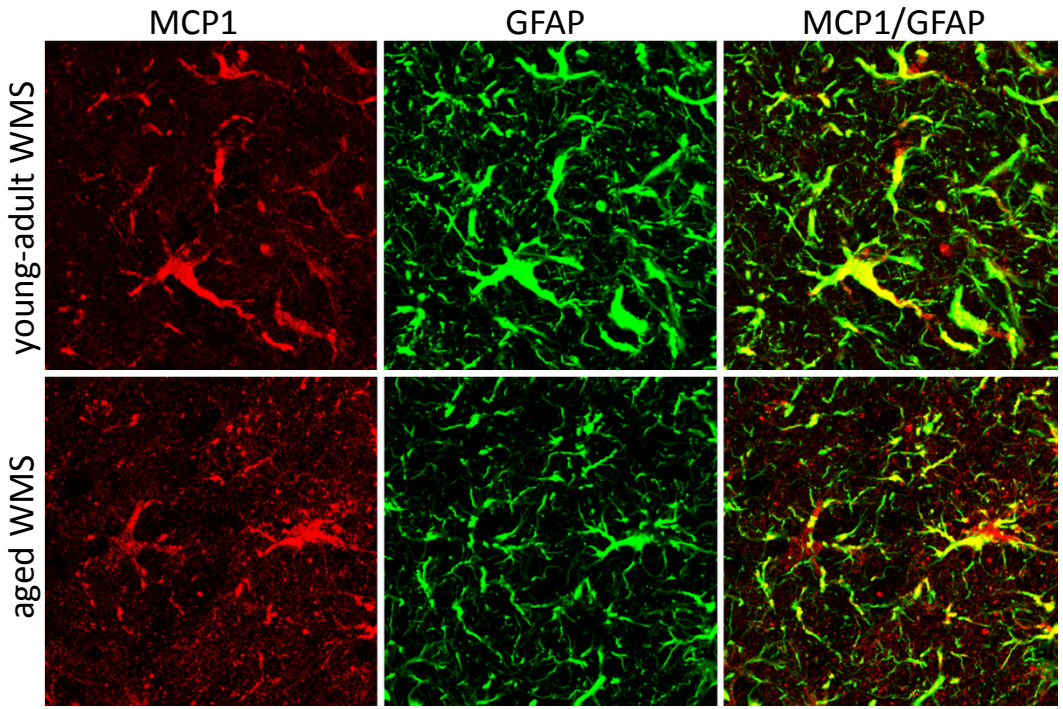
MCP1
GFAP
MCP1/GFAP
young-adult WMS
aged WMS

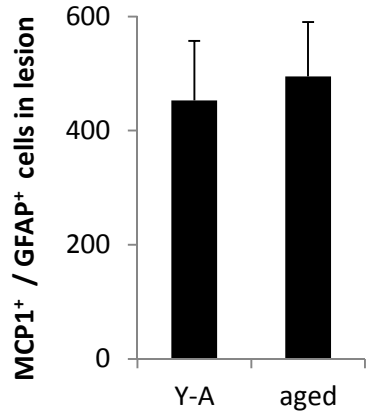
MCP1+ / GFAP+ cells in lesion
600
400
200
0
Y-A
aged

SUPPLEMENTAL MATERIAL

Age-dependent exacerbation of white matter stroke outcomes: a role for oxidative damage and inflammatory mediators

The Supplementary Material includes the following:

1. Supplementary Methods

I. Tissue Processing for TUNEL and Immunohistochemistry

Animals were perfused transcardially with 0.1 M phosphate buffered saline followed by 4% paraformaldehyde. Following cryoprotection in 30% sucrose brains were frozen and sectioned using a cryostat (Leica CM 0530) into 20-35µm sections. For Iba-1, NF200, MBP and Olig2 immunostaining, the sections were blocked in 5% donkey serum, incubated with a primary antibody over night at 4°C, incubated with a secondary antibody for 1-2 hours at room temperature, and coverslipped with DPX. Primary antibodies were: rabbit anti Iba-1 (1:1000, Wako Chemicals) rabbit anti-NF200 (1:1000, Sigma) rat anti-myelin basic protein (MBP, 1:1000, Millipore), rabbit anti Olig2 (1:500, Millipore), mouse anti-8-OHdG (1:100, Abcam), rat anti-neutrophil (1:100, Abcam), rabbit anti-MCP1 (1:500, Novus Biologicals), goat anti-TNFα (1:500, R&D Systems), rat anti-GFAP (1:500, Millipore). All secondary antibodies were donkey F(ab)2 fragments conjugated to cy2 or cy3 (Jackson Immunoresearch) and were used at a dilution of 1:500. TUNEL assay was performed using ApopTag® In Situ Apoptosis Detection Kit (S7110, Millipore). Briefly, sections were incubated with terminal deoxynucleotidyl transferase which catalyzes the addition of nucleotide triphosphates labeled with digoxigenin to the 3'-OH ends of double-stranded or single-stranded DNA (which localize in apoptotic bodies in high concentrations). The digoxigenin was then detected with an antibody conjugated to fluorescein. Nuclear stains were performed by incubating the sections for 5 minutes in phosphate-buffered saline containing either DAPI or propidium iodide before coverslipping.

II. Quantification of NF200-positive axons

Analysis of corticostriatel projections was performed in high-resolution confocal images and Z-stacks of sections stained for the axonal marker NF200. To quantify the axonal loss, intensity profiles were created for 0.5x0.7mm areas in the dorsomedial striatum (sample regions of interest outlined in Figure 5A with corresponding ImageJ plot profiles in Figure 5B). Peak grey values were added across plots to yield the cumulative NF200 intensity for the regions of interest (Figure 5C).

III. Behavior

The pasta matrix task was performed as described previously [1, 2]. In this task, mice reach through a window to retrieve small pieces (3.3 cm in height and 1 mm diameter) of vertically-oriented capellini pasta from a grid arrangement on a shelf in front of the animal. Mice were trained daily on the task for 5 weeks before stroke. The number of pasta breaks per 10-minute daily session was averaged across two consecutive days of training. Acquisition of the task was defined as a >4 average with a standard deviation <6 of breaks. Mice that failed to learn the task after 5 weeks of training were excluded from the study. Following the stroke the mice were tested weekly, on two consecutive days each week, for 8 weeks. Performance on the two days of testing

each week was averaged and compared to the pre-stroke performance (each mouse was compared to its baseline pre-stroke performance). The grid-walking task was performed as previously described [3-5]. The total number of footfaults as well as the total number of correct, non-footfault steps were counted, and a correct step percentage was calculated. Mice were tested in the grid-walking task once before the stroke to establish baseline performance levels, and then re-tested 1 week, one month and two months following the stroke.

2. Supplementary Figures

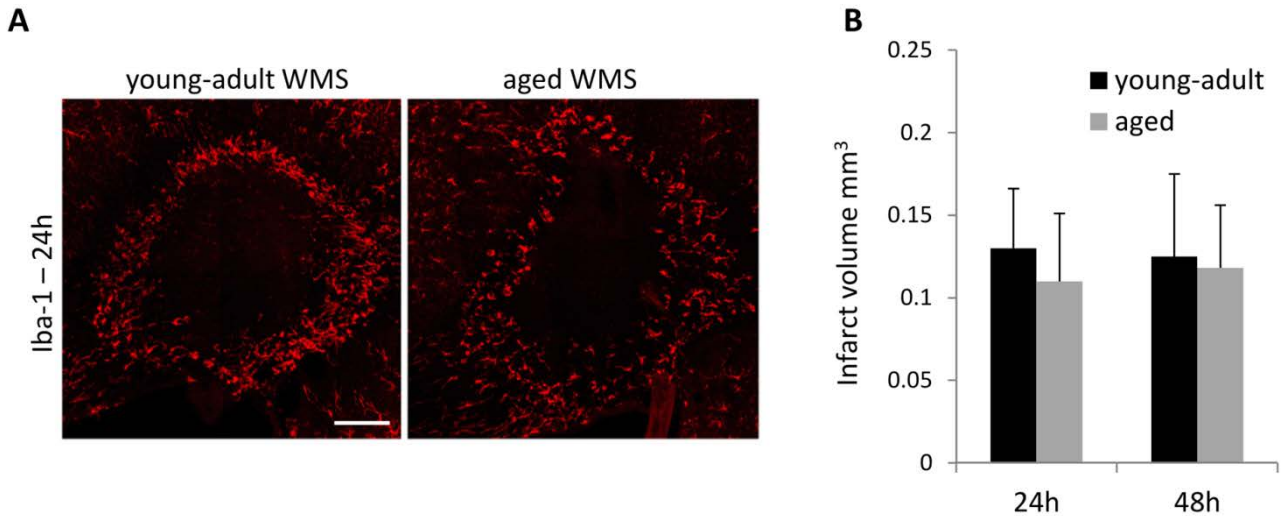

Supplementary Figure I. Infarct volume 24 hours after WMS. The infarct core is defined in the white matter by surrounding microglia (red) expressing Iba-1. Scale bar = 50μm (A). Similar infarct volume between young adult and aged animals 24h after WMS (B).

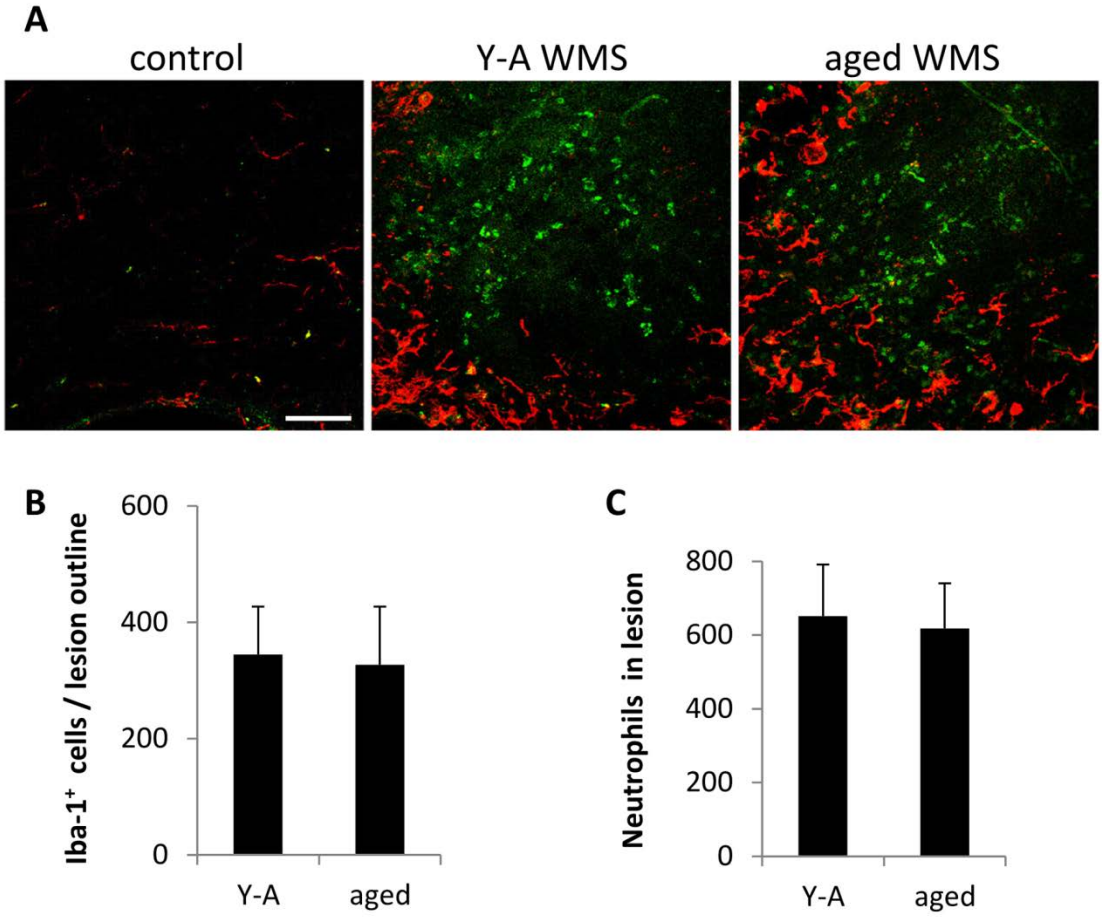

Supplementary Figure II. Reactive microglia and neutrophil infiltration 24 hours after WMS. Iba-1-positive microglia (red) are present around the outline of the lesion, while Ly6G-positive neutrophils (green) can be detected throughout the lesion core. Scale bar = 20µm (A). Similar numbers of microglia and neutrophils in young-adult and aged mice 24h after WMS (B,C).

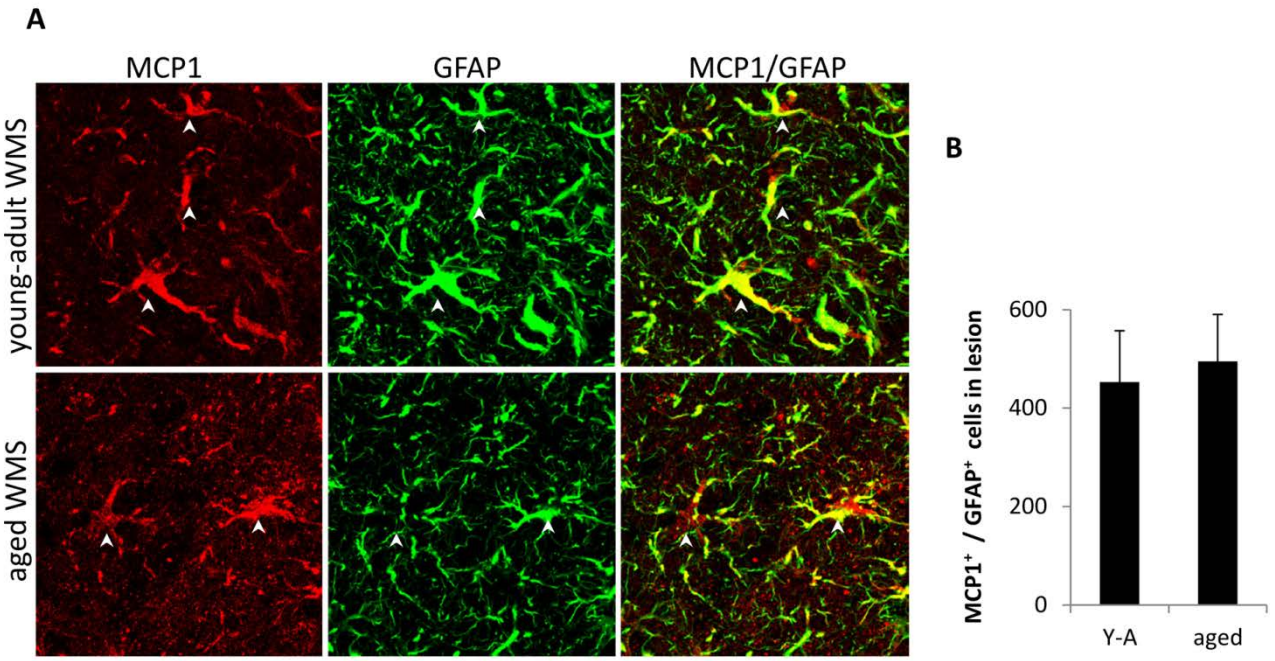

Supplementary Figure III. MCP1 expression in infarct core 7 days after WMS. GFAP-positive astrocytes (green) express MCP1(red). Similar numbers of MCP1-expressing astrocytes in young-adult and aged mice 7 days after WMS (B).

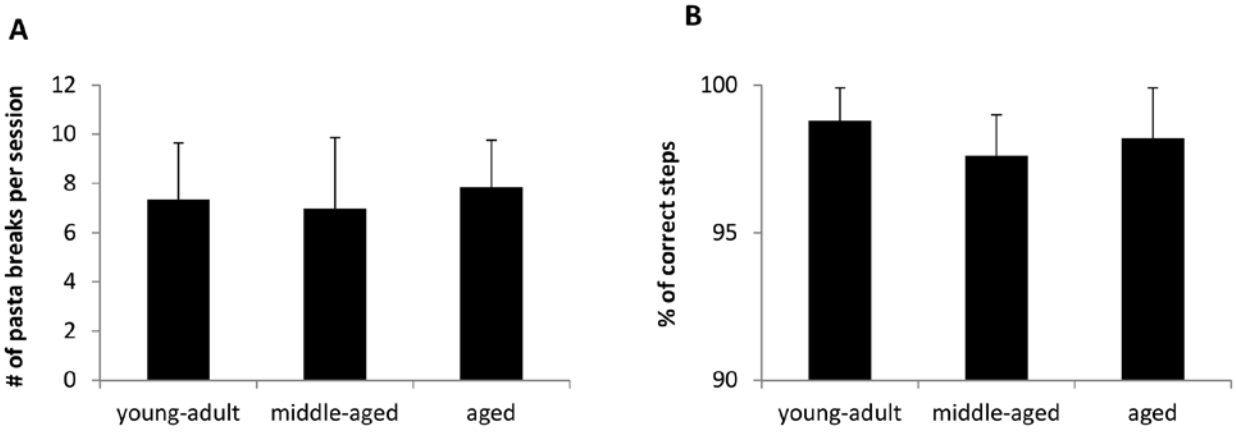

Supplementary Figure IV. Baseline performance in behavioral tests. Pasta matrix reach task: average number of pasta breaks for a 10-minute session before WMS was similar between age groups (A). Grid-walking task: percent of correct steps in a 10-minute session was similar between age groups.

3. References

1. Tennant KA, Jones TA. Sensorimotor behavioral effects of endothelin-1 induced small cortical infarcts in c57bl/6 mice. *Journal of neuroscience methods*. 2009;181:18-26
2. Tennant KA, Adkins DL, Scalco MD, Donlan NA, Asay AL, Thomas N, et al. Skill learning induced plasticity of motor cortical representations is time and age-dependent. *Neurobiology of learning and memory*. 2012;98:291-302
3. Clarkson AN, Huang BS, Macisaac SE, Mody I, Carmichael ST. Reducing excessive gaba-mediated tonic inhibition promotes functional recovery after stroke. *Nature*. 2010;468:305-309
4. Clarkson AN, Overman JJ, Zhong S, Mueller R, Lynch G, Carmichael ST. Ampa receptor-induced local brain-derived neurotrophic factor signaling mediates motor recovery after stroke. *The Journal of neuroscience : the official journal of the Society for Neuroscience*. 2011;31:3766-3775
5. Overman JJ, Clarkson AN, Wanner IB, Overman WT, Eckstein I, Maguire JL, et al. A role for ephrin-a5 in axonal sprouting, recovery, and activity-dependent plasticity after stroke. *Proceedings of the National Academy of Sciences of the United States of America*. 2012;In press.